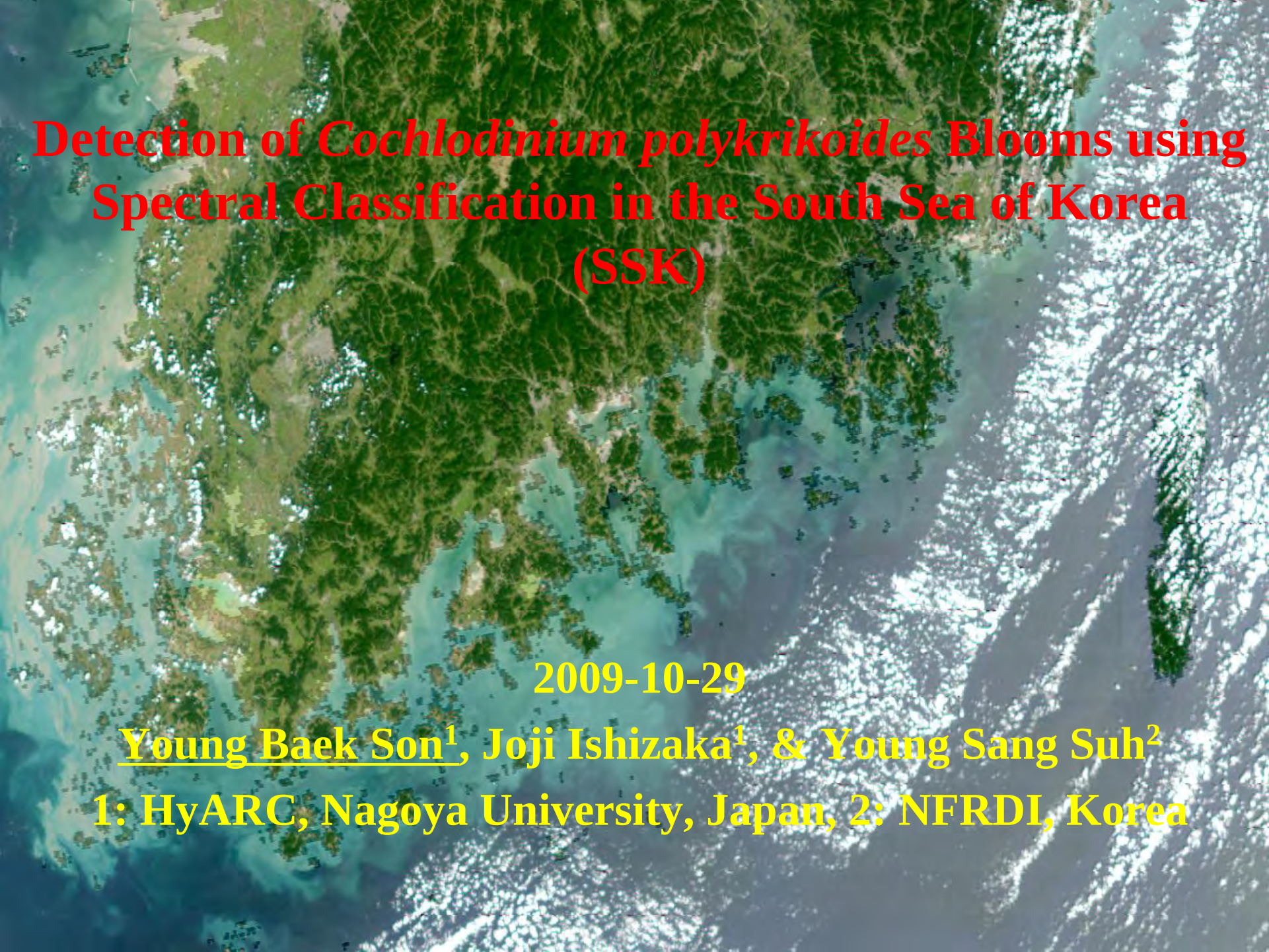

Detection of *Cochlodinium polykrikoides* Blooms using Spectral Classification in the South Sea of Korea (SSK)

2009-10-29

Young Baek Son[1], Joji Ishizaka[1], & Young Sang Suh[2]

1: HyARC, Nagoya University, Japan, 2: NFRDI, Korea

Red Tide : Detection From Space

After 1995 : *C. polykrikoides* Blooms

Before 1995

Diatom Blooms

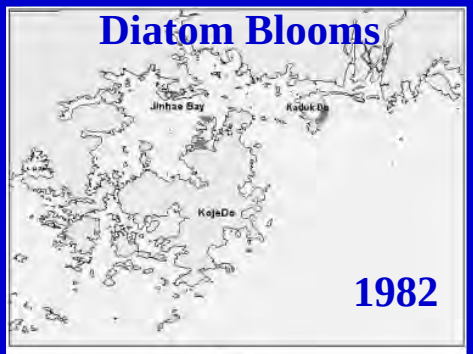

1982

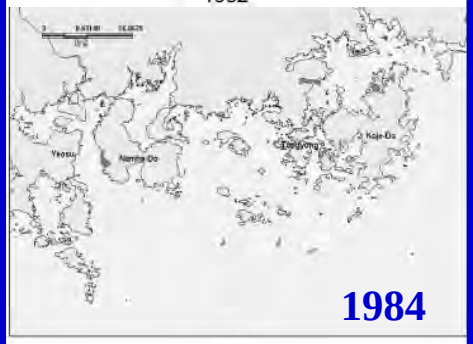

1984

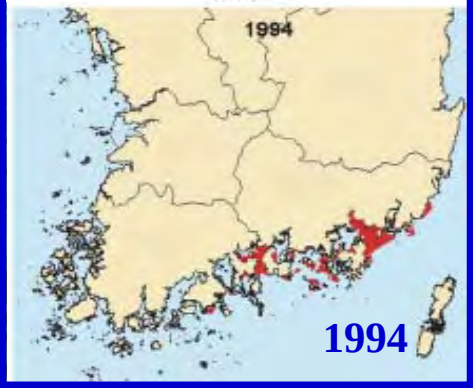

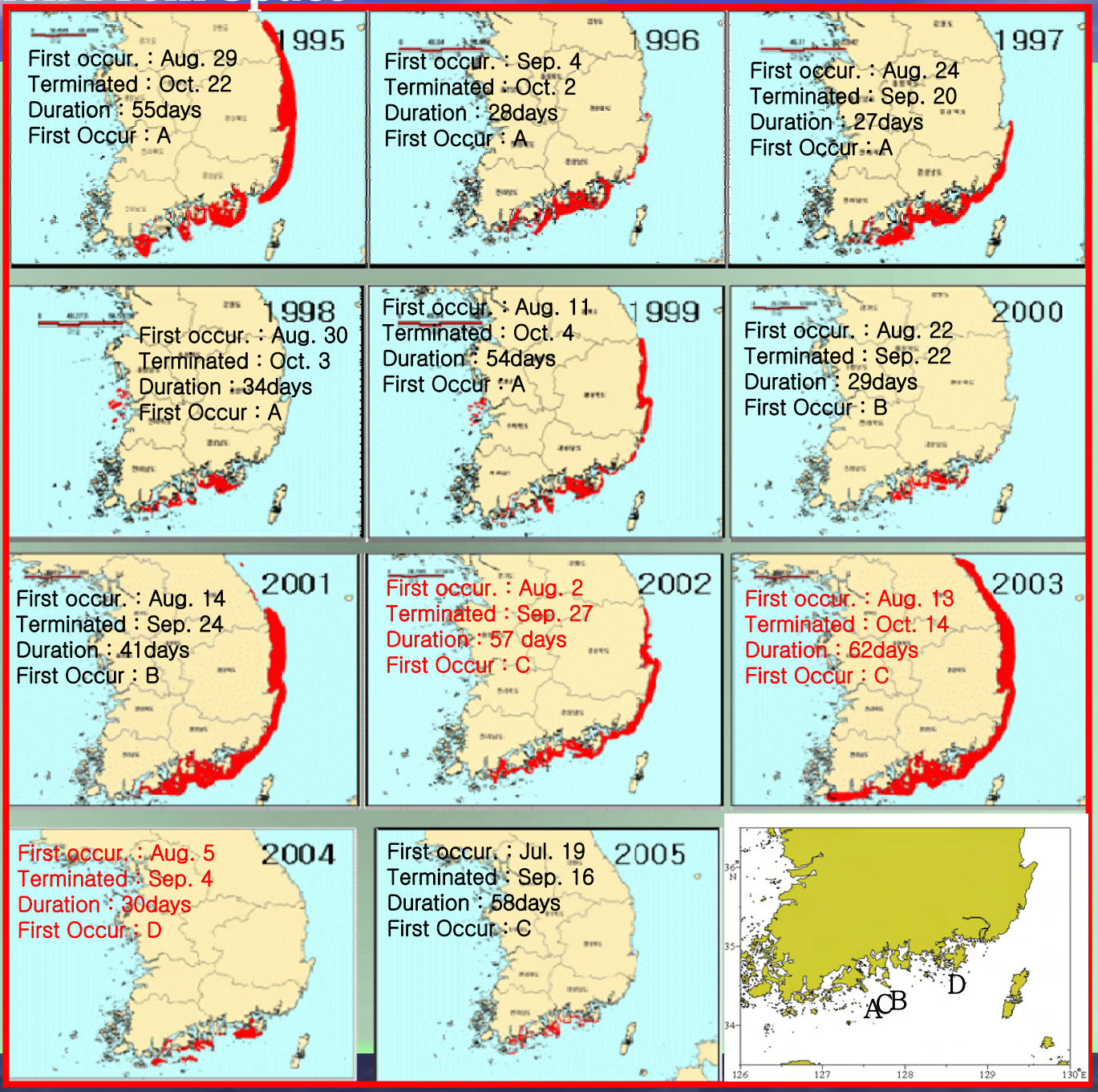

Red Tide : Detection From Space

1. Ishizaka, et al 2006. Satellite Detection of Red Tide in Ariake Sound, 1998-2001, J. Oceanog. 62, 37-45.

Rhizosolenia imbricata, complex waters in Ariake Sound, SeaWiFs

Monthly averaged image of Chl-a OC4 : two peaks of high Chl-a, summer and late fall related to monthly precipitation and discharge of Chikugo River

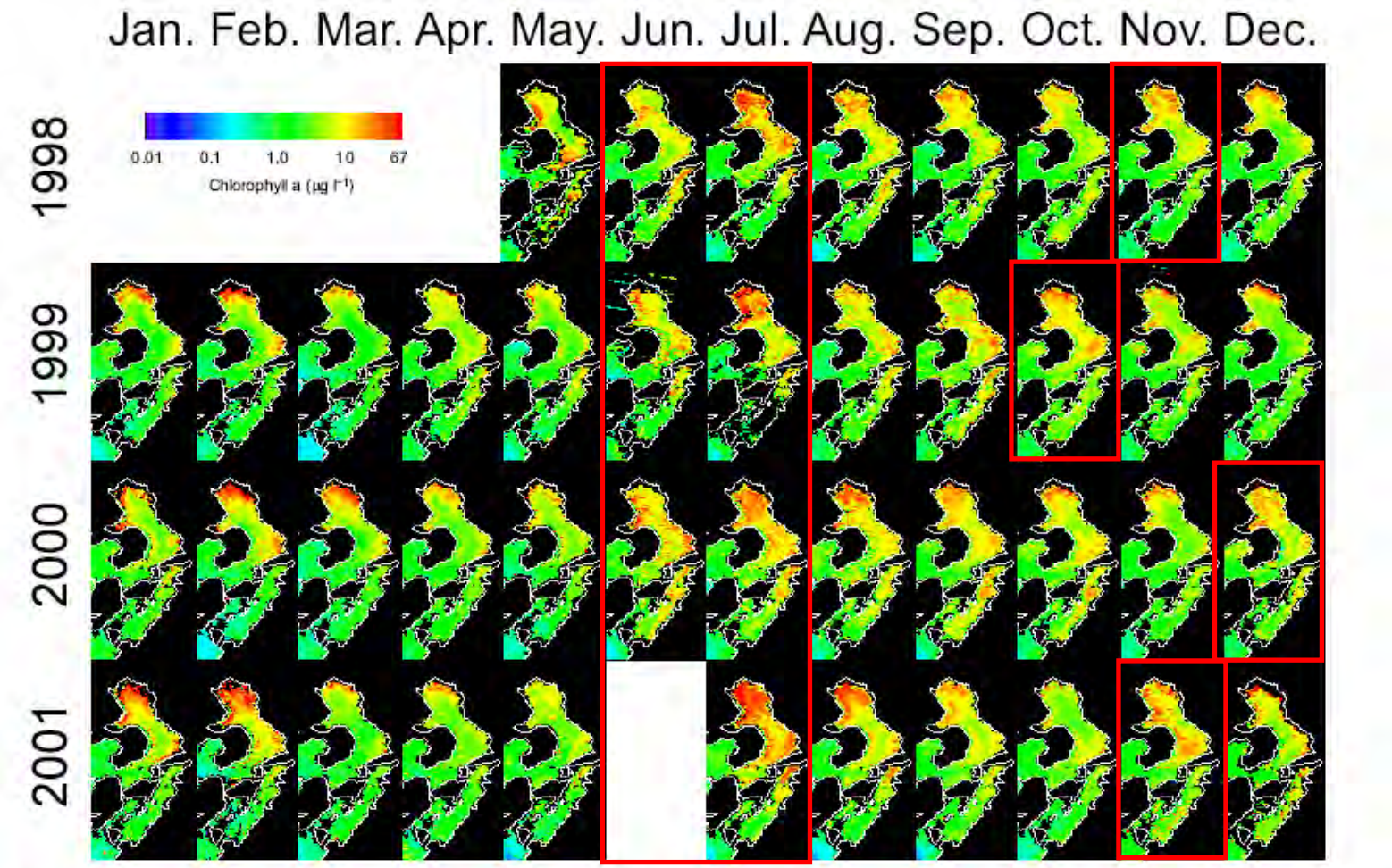

Fig. 7. Monthly SeaWiFS chlorophyll distribution in Ariake Sound during 1999–2001. Color scale is as in Fig. 2.

Red Tide : Detection From Space

2. Stumpf, et al, 2003, Monitoring *Karenia brevis* blooms in the Gulf of Mexico using satellite ocean color imagery and other data. Harmful Algae, 2, 147-160.
3. Tomlinson et al., 2004, Evaluation of the use of SeaWiFS imagery for detecting *Karenia brevis* harmful algal blooms in the eastern Gulf of Mexico, Remote Sens. Environ., 91, 293-303.

➔ Standard Chl-a Algorithm, anomaly from averaged 2 month.

➔ Frequently False signal in the spring and early summer due to high CDOM and PM

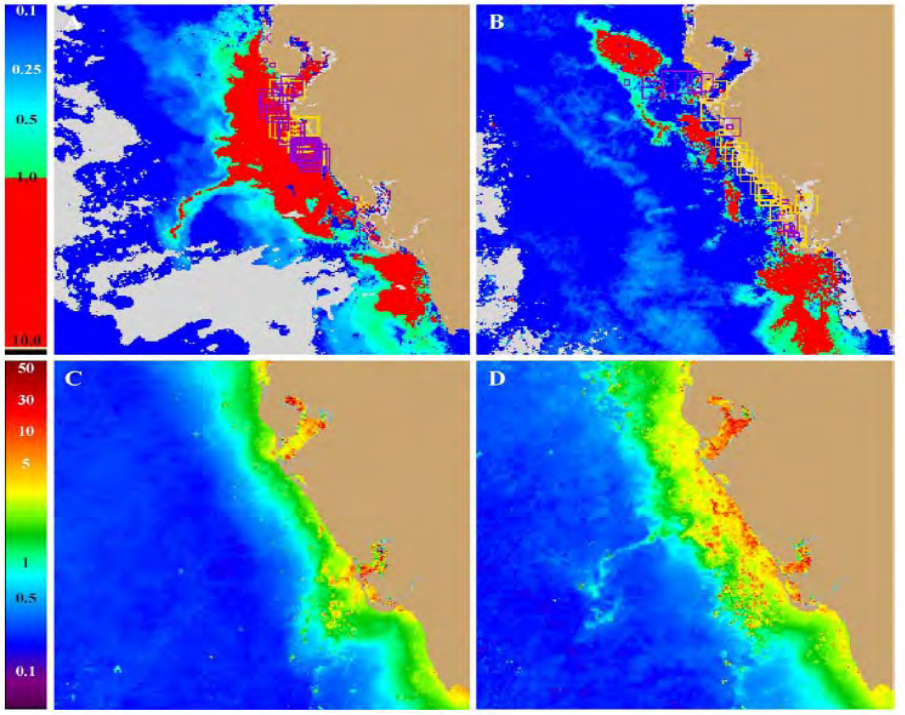

Fig. 6. Chlorophyll anomaly images for (A) September 17 and (B) November 7, 2001, following the passage of Tropical Storm Gabrielle. Cell concentrations are shown by symbol size: large squares are 10^6 cells l^{-1} and above; medium squares are from 10^5 to $<10^6$ cells l^{-1}; medium-low squares represent 10^3 to $<10^5$ cells l^{-1}; small squares represent cell counts $<10^3$ cells l^{-1}. The crosses indicate no cells. The symbol color represents the time lag in cell count data, from the imagery. Yellow is within ± 1 day and purple squares represent -2 to -3 days. Red areas within imagery represent chlorophyll anomalies exceeding 1 µg l^{-1}. Bottom images show the 60-day mean chlorophyll used to compute anomalies for (C) September 17 (mean from July 6 through September 2, 2001) and (D) November 7, 2001 (mean from August 27 through October 17, 2001).

Red Tide : Detection From Space

4. Hu, et al, 2005. Red tide detection and tracing using MODIS fluorescence data : A regional example in SW Florida coastal waters, Remote Sens. Environ. 97, 311-321.
MODIS fluorescence (665,676,746 nm) for detecting and tracing of HABs,
True color image using 551(red), 488 (green), 443 (blue) nm, Chl = $1.255(FLHx10)^{0.86}$

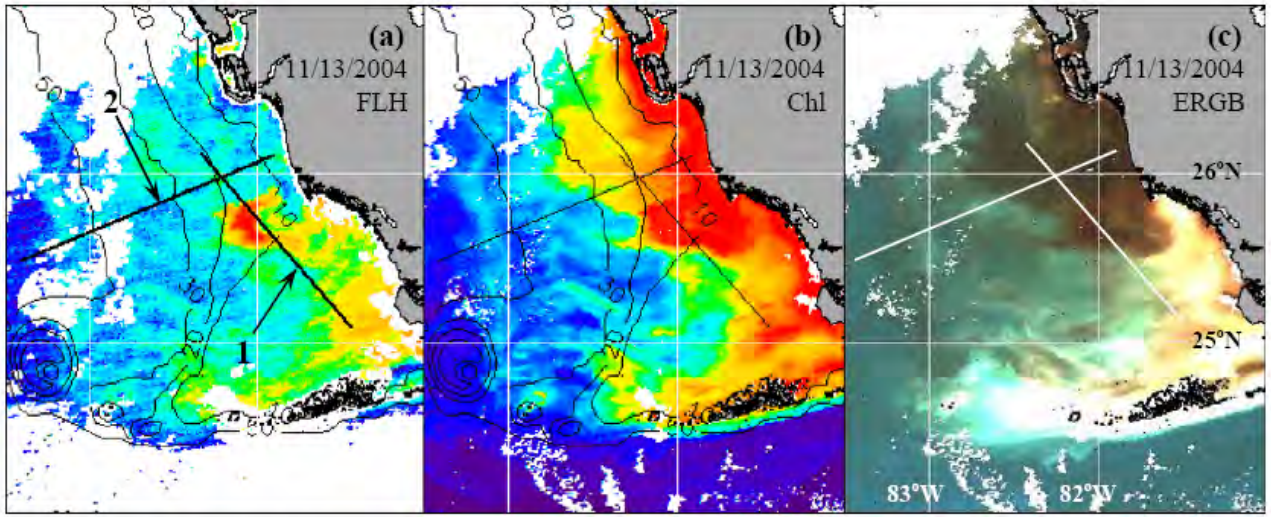

Fig. 4. Similar to Fig. 1, but MODIS/Aqua imagery was obtained on 13 November 2004 (18:32 GMT). Color scales can be found in Fig. 1. Overlaid on the FLH and Chl images are two arbitrary along-coast and cross-shelf transect lines used to extract several parameters (shown in Fig. 5).

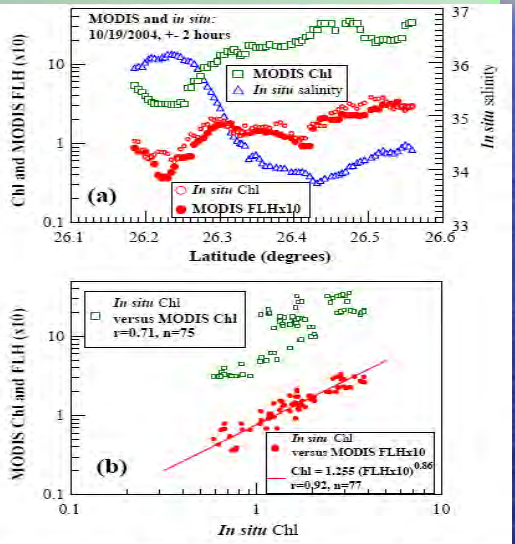

Fig. 2. Biological and physical parameters measured using MODIS and in situ surveys within ±2 h of each other. (a) In situ Chl (mg m^{-3}; calibrated fluorescence data) and salinity, plus MODIS FLH (W m^{-2} μm^{-1} sr^{-1}; to facilitate visual comparison with other properties a factor of 10 was used to construct the figure) and MODIS Chl (mg m^{-3}) along the transect line in Fig. 1a; (b) In situ Chl *vs.* MODIS FLH and MODIS Chl along the transect line. Solid line is the regression between in situ Chl and MODIS FLH.

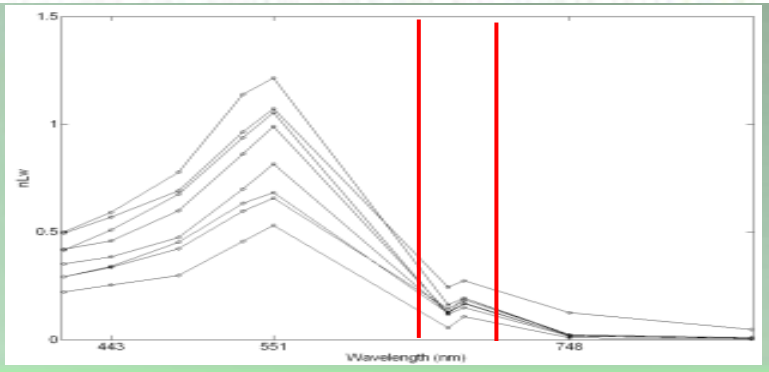

Red Tide : Detection From Space

1. HAB conditions would be well correlated with chlorophyll *a* concentrations.
2. but often estimated as the false signal due to influence of CDOM and suspended materials which inaccurately estimated as high chlorophyll concentrations.
3. The FLH approach was simply used to the bottom-line approach using MODIS three bands whether a radiance peak was at 678 nm or not.

   => it led to be problem with high suspended particulate materials due to increasing interaction between chlorophyll and suspended material.

The objective of this study :

1. to identify the spectral characteristics of red tide (specifically *C. polykrikoides* bloom) using radiance, satellite chlorophyll *a* concentration, FLH and IOP derived from MODIS ocean color data,
2. to discriminate red tide water from non-red tide water, and then
3. to finally delineate temporal and spatial variability of HABs in various water conditions.

2. Methods and Data: To detect/monitor the huge blooms from space

1) Five MODIS satellite data were matched with in-situ red tide information (NFRDI).

2) MODIS satellite products :

- the spectral normalized water-leaving radiance (nLw),
- satellite chlorophyll concentration (Chlor-a),
- fluorescence line height (FLH),
- phytoplankton absorption (a_{ph}) and CDOM (Detritus) absorption (a_{dg}),
- particle backscattering coefficients (b_p).

3) ~ 300 satellite sub-sample data collected from red tide areas :

- the spectral response of various water mass and red tide signals
- the red and non-red tide waters -> spectral classification and band ratio.

4) Demonstrates how the improved discrimination in mapping HAB distributions.

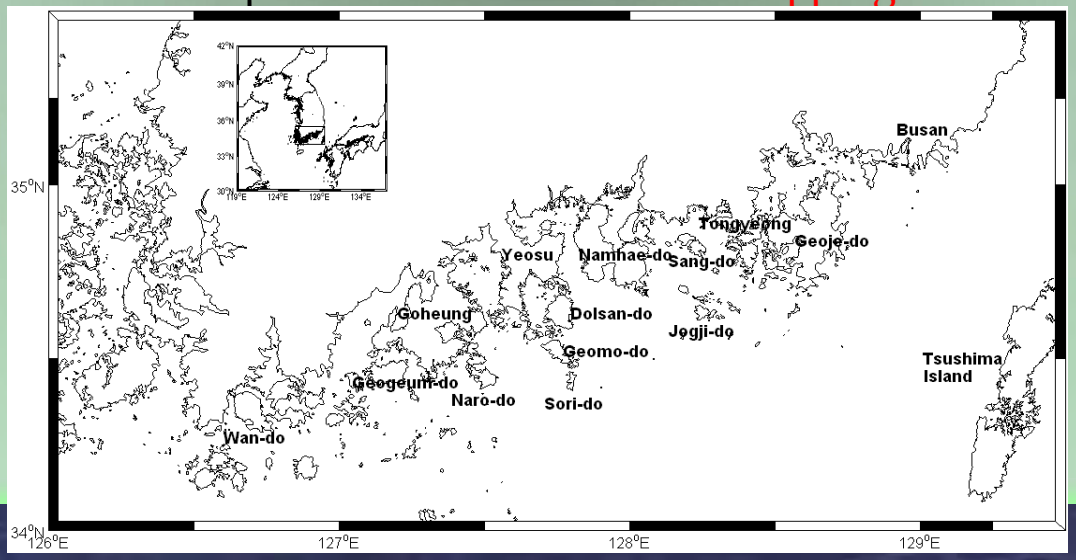

3. Results

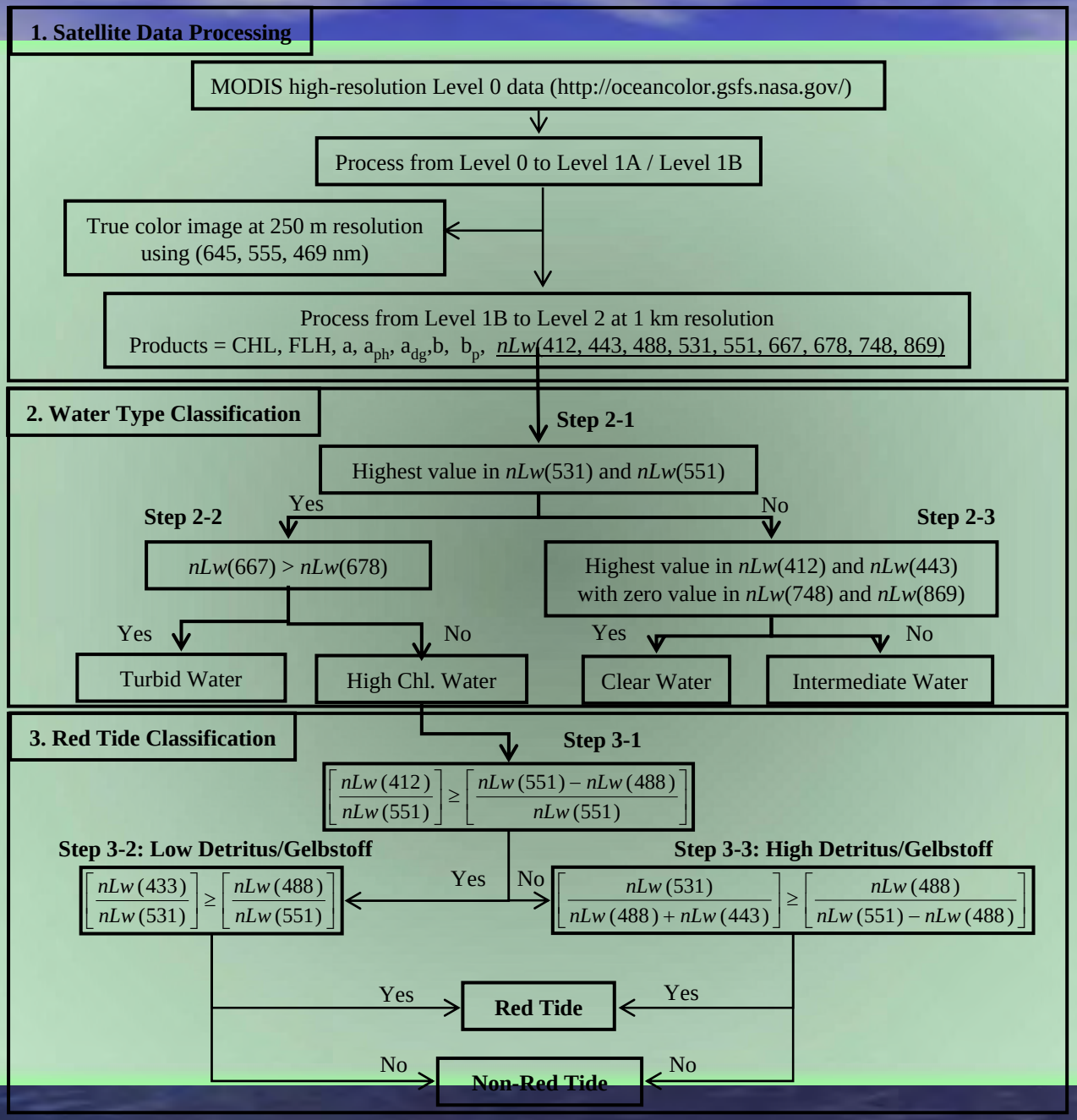
1. Satellite Data Processing
MODIS high-resolution Level 0 data (http://oceancolor.gsfs.nasa.gov/)
Process from Level 0 to Level 1A / Level 1B
True color image at 250 m resolution using (645, 555, 469 nm)
Process from Level 1B to Level 2 at 1 km resolution
Products = CHL, FLH, a, a_{ph}, a_{dg},b, b_p, nLw(412, 443, 488, 531, 551, 667, 678, 748, 869)
2. Water Type Classification
Step 2-1
Highest value in nLw(531) and nLw(551)
Yes
No
Step 2-2
Step 2-3
nLw(667) > nLw(678)
Highest value in nLw(412) and nLw(443) with zero value in nLw(748) and nLw(869)
Yes
No
Yes
No
Turbid Water
High Chl. Water
Clear Water
Intermediate Water
3. Red Tide Classification
Step 3-1
$\left[\frac{nLw(412)}{nLw(551)}\right] \geq \left[\frac{nLw(551)-nLw(488)}{nLw(551)}\right]$
Step 3-2: Low Detritus/Gelbstoff
Step 3-3: High Detritus/Gelbstoff
$\left[\frac{nLw(433)}{nLw(531)}\right] \geq \left[\frac{nLw(488)}{nLw(551)}\right]$
Yes
No
$\left[\frac{nLw(531)}{nLw(488)+nLw(443)}\right] \geq \left[\frac{nLw(488)}{nLw(551)-nLw(488)}\right]$
Yes
Red Tide
Yes
No
Non-Red Tide
No

3. Results : Water Type Classification

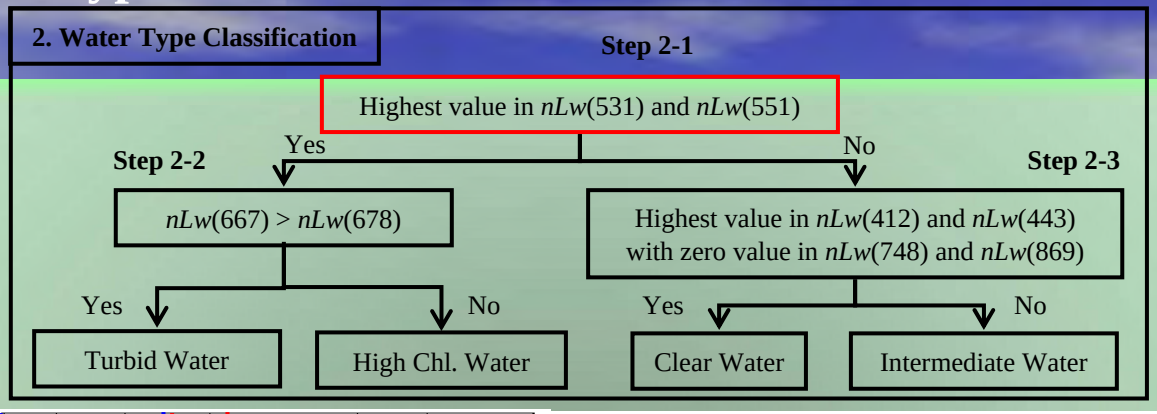

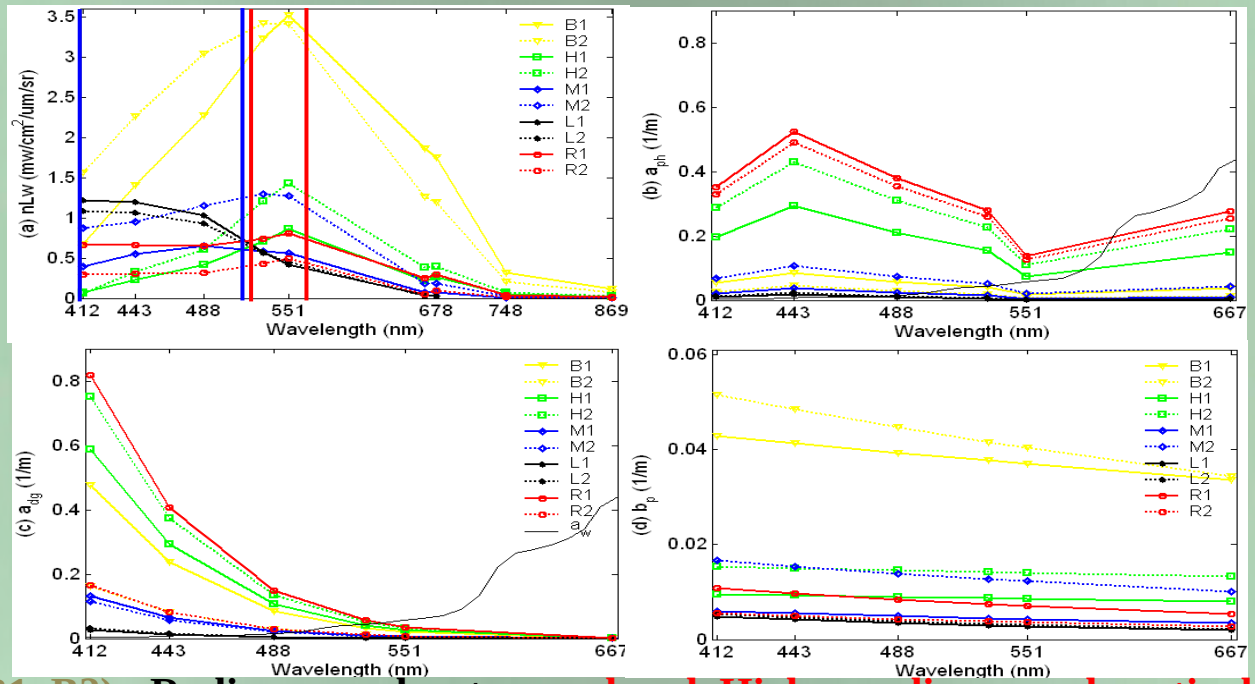

Bright color (B1, B2) : Radiance peaks at green band. Higher radiance and particulate backscattering but phytoplankton absorption is minimal

High chlorophyll and red tide (H, R) : Radiance peaks at green band. Higher absorption of the phytoplankton and gelbstoff/detritus . Particulate backscattering values are ~3-4 times lower than in bright color samples.

3. Results : Water Type Classification

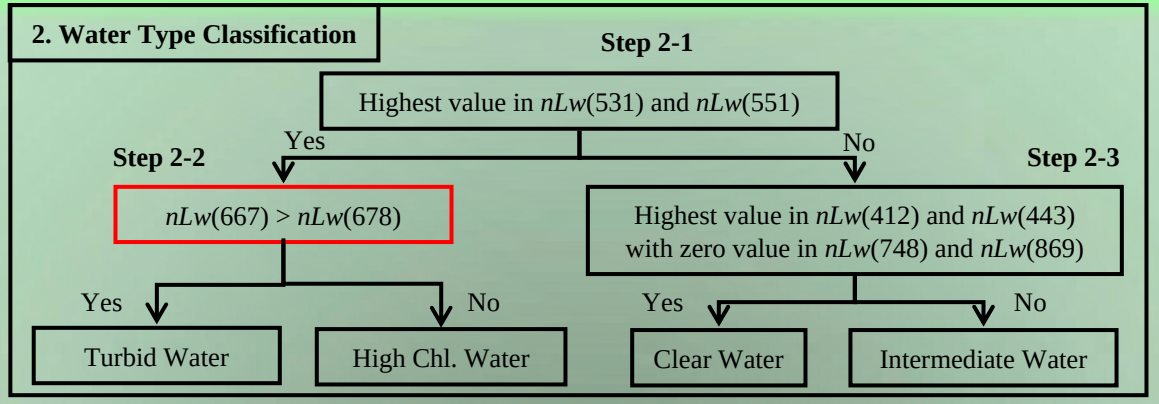

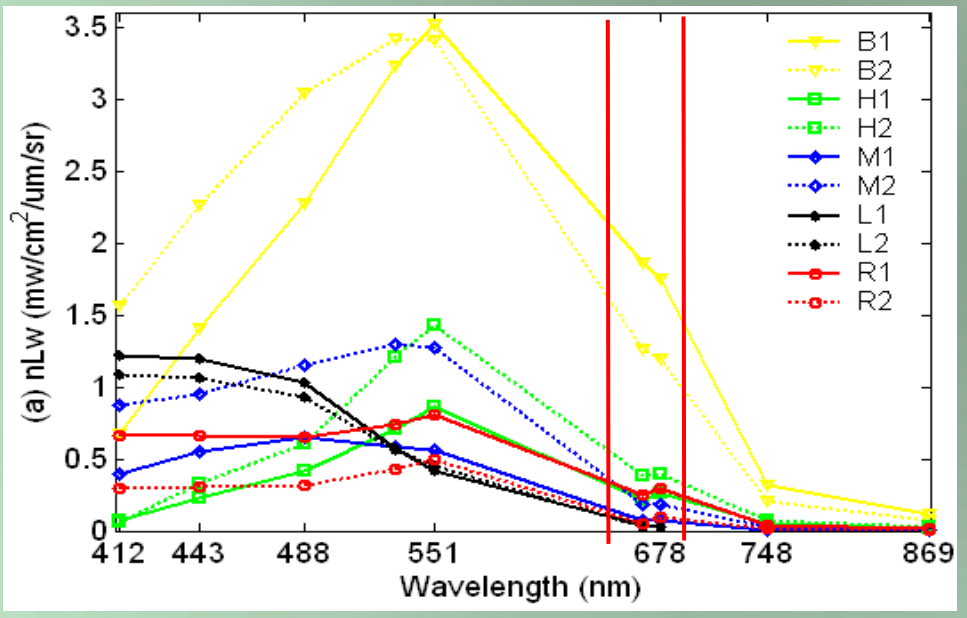

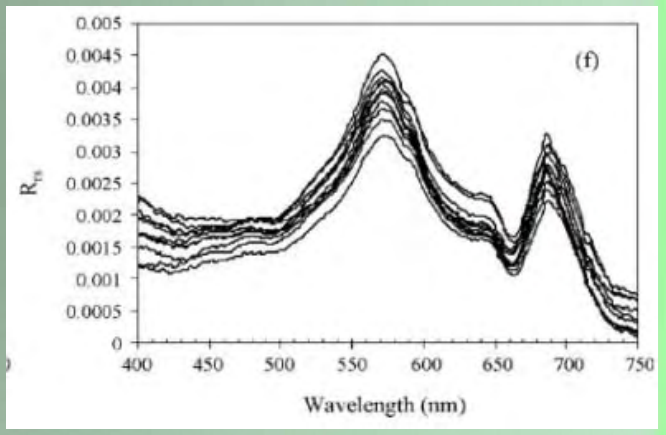

Weak fluorescence signals disappeared through surface turbid water column due to complex interactions with suspended particulate materials (Ahn and Shanmugam, 2006; Babin et al., 1996)

3. Results : Water Type Classification

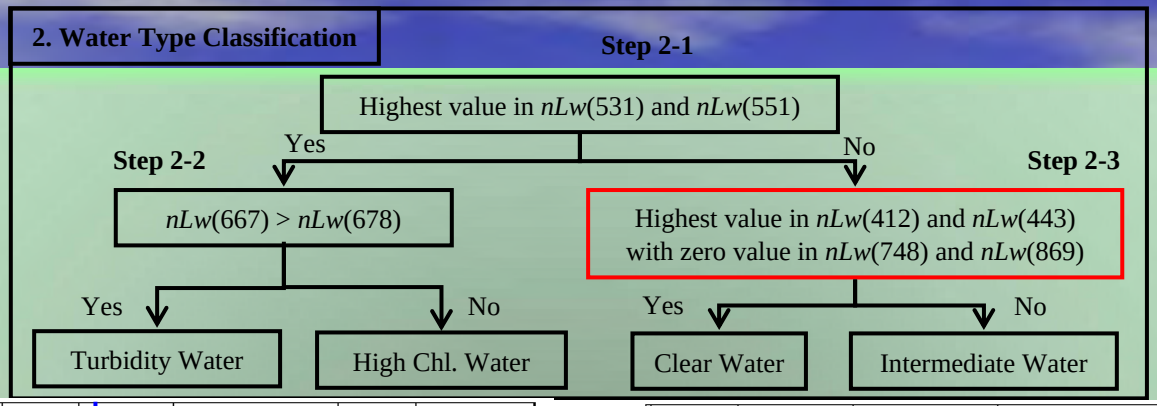

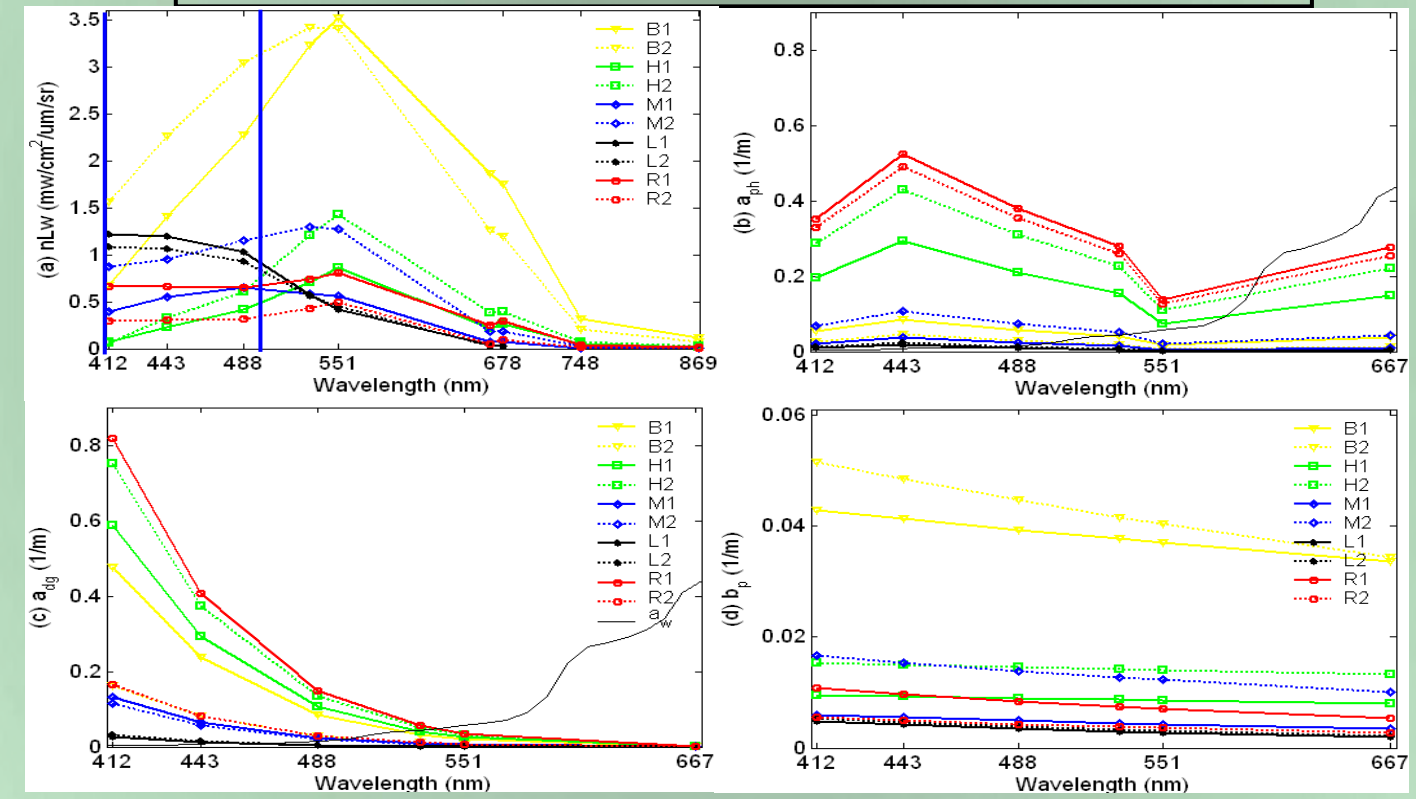

Low and moderate chlorophyll (L, M) : Radiance peaks from 412 nm to 531 nm (blue to green bands)
absorption and backscattering of the phytoplankton, gelbstoff, and detritus in all visual wavelengths

3. Results : Red Tide Classification

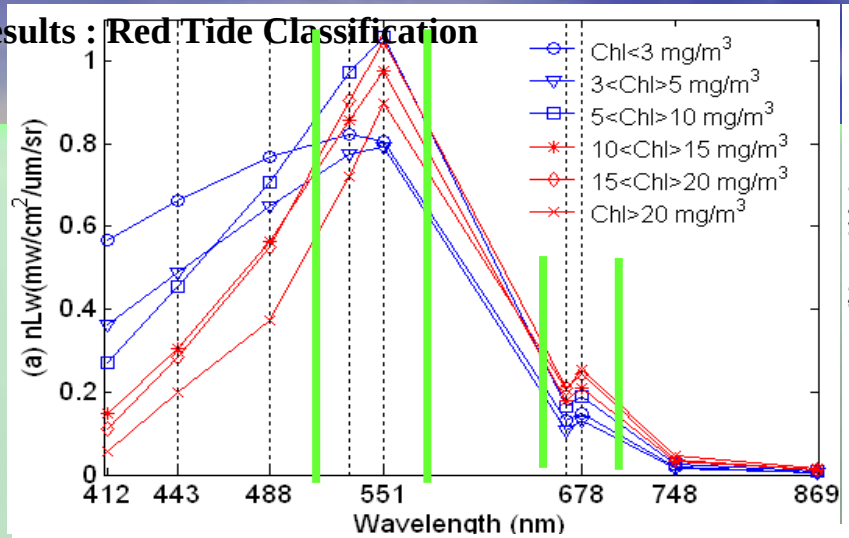

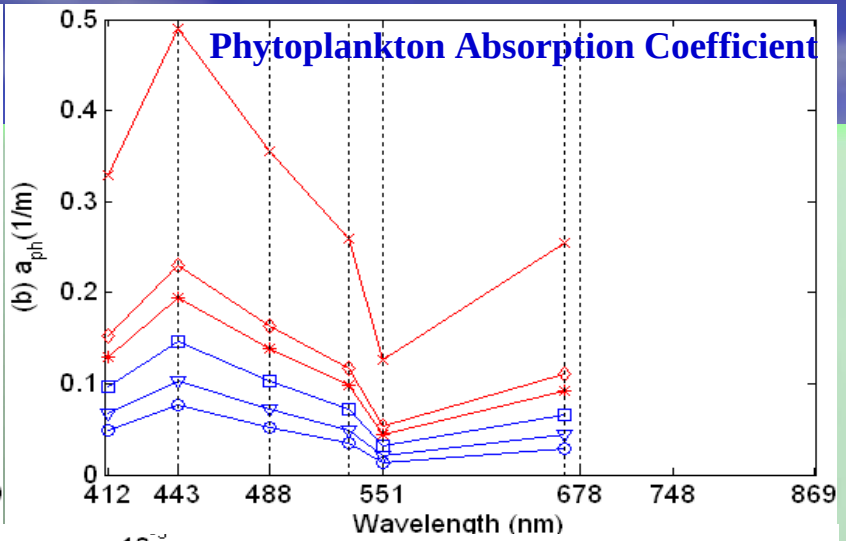

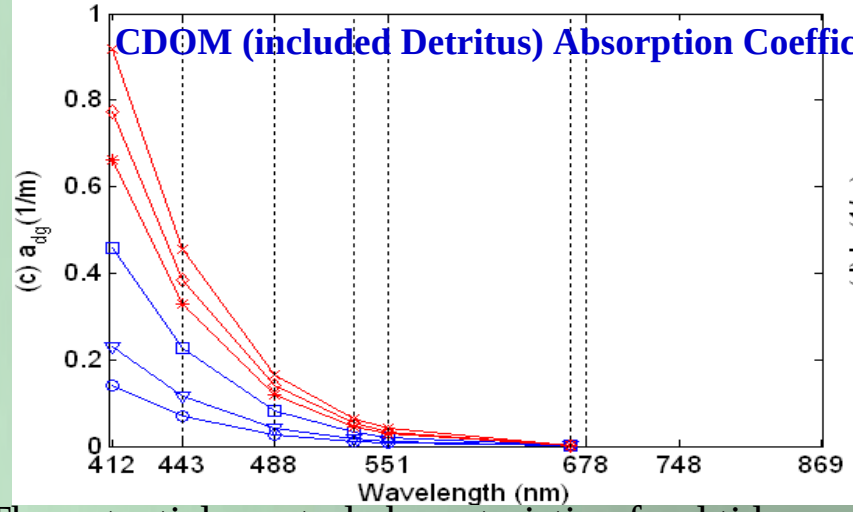

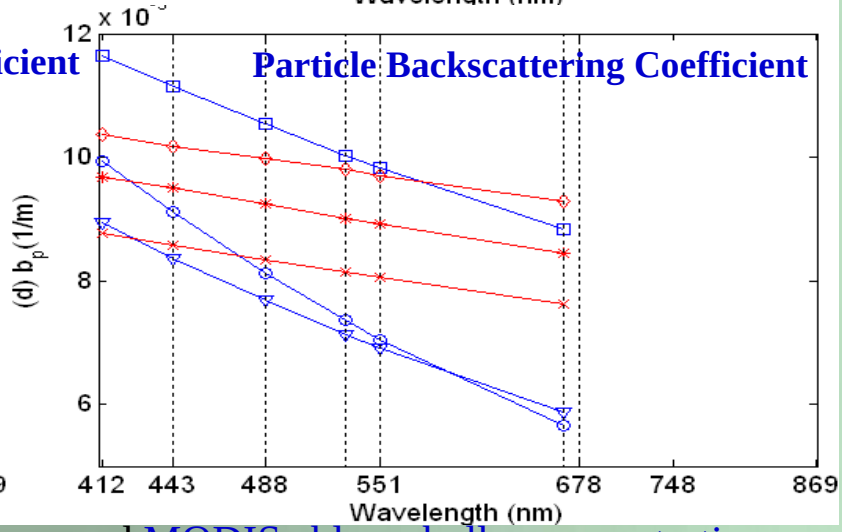

1. The potential spectral characteristic of red tide : averaged MODIS chlorophyll-a concentration.
2. Radiance spectra : two dominant peaks at 531/551 (green bands) and 678 (red band) nm.
3. Low value at blue wavelengths (> 10 mg m^{-3} : red line) : high phytoplankton and detritus/gebstoff absorptions and small difference between blue and red bands
4. High value at blue bands (< 10 mg m^{-3} : blue line) : low phytoplankton and detritus/gebstoff absorptions and high difference between blue and red bands.

3. Results : Red Tide Classification

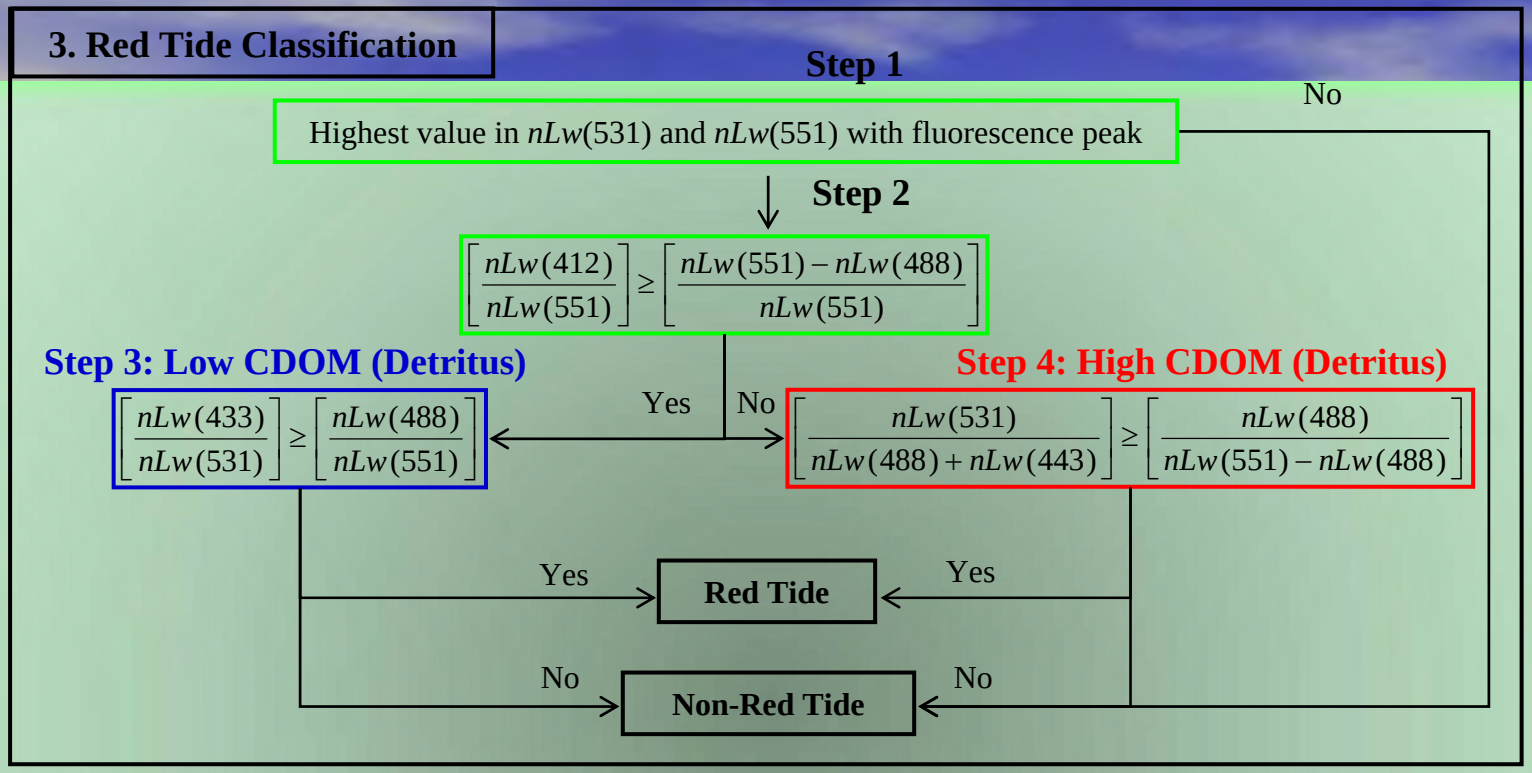

1. *C. polykrikoides* blooms :

- Onshore (high influence of CDOM or organic/inorganic material, increasing absorption in blue bands)
- Offshore (less influence of CDOM or organic/inorganic material, decreasing absorption and increasing water backscattering in blue bands).

2. Step 2 : Relatively high and low contribution of detritus/gelbstoff to chlorophyll

3. Step 3 : Lower contribution of CDOM to chlorophyll

4. Step 4 : Higher contribution of CDOM to chlorophyll

3. Results : Low effect of Detritus/gelbstoff

Blue Color :

$$\left[\frac{nLw(443)}{nLw(531)}\right] \geq \left[\frac{nLw(488)}{nLw(551)}\right]$$

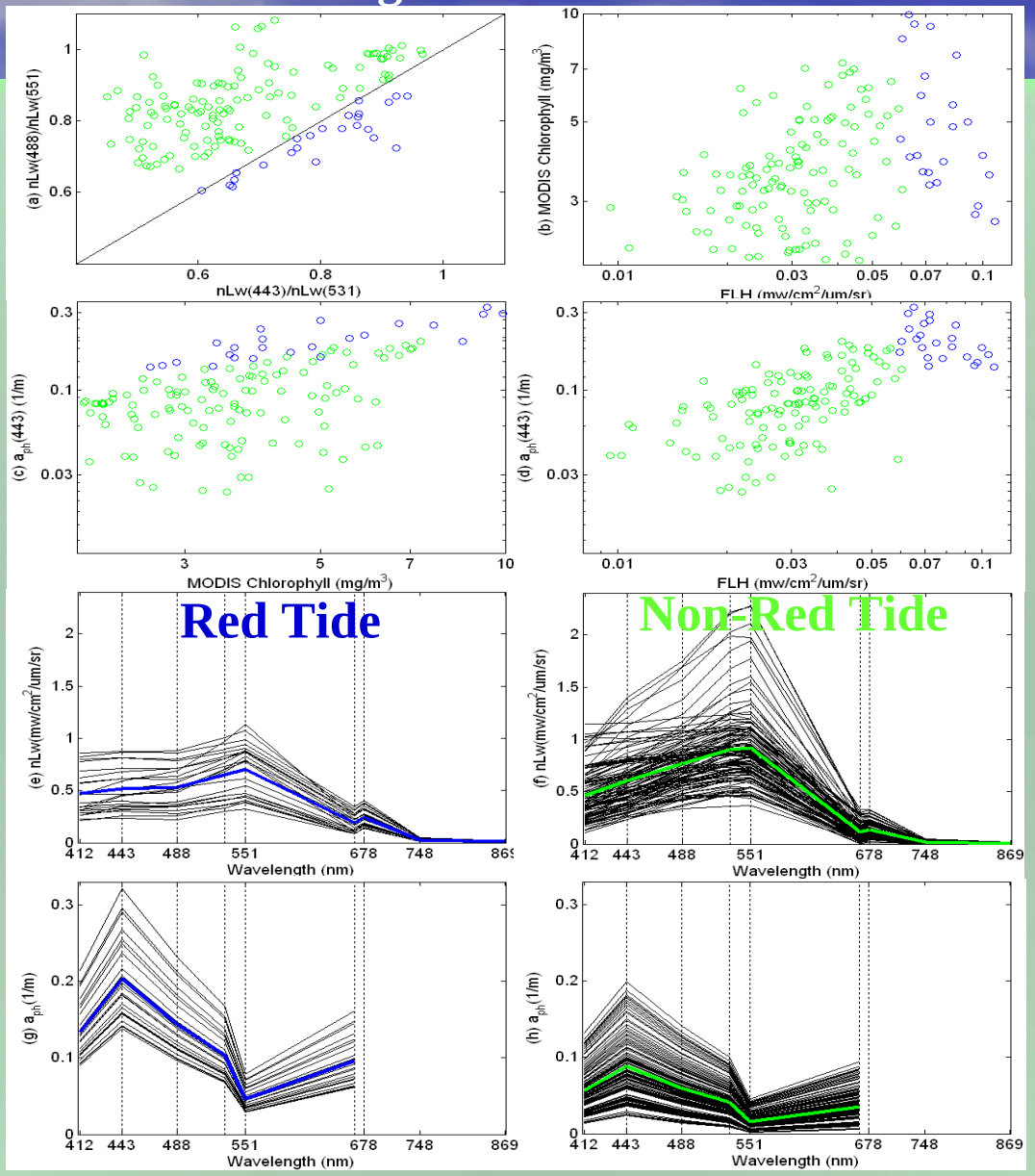

Green Color :

$$\left[\frac{nLw(443)}{nLw(531)}\right] < \left[\frac{nLw(488)}{nLw(551)}\right]$$

1. **Red tide : relative high FLH and phytoplankton absorption values.**

2. **Non-red tide : relative low FLH and phytoplankton absorption values.**

3. Results : Red Tide Classification

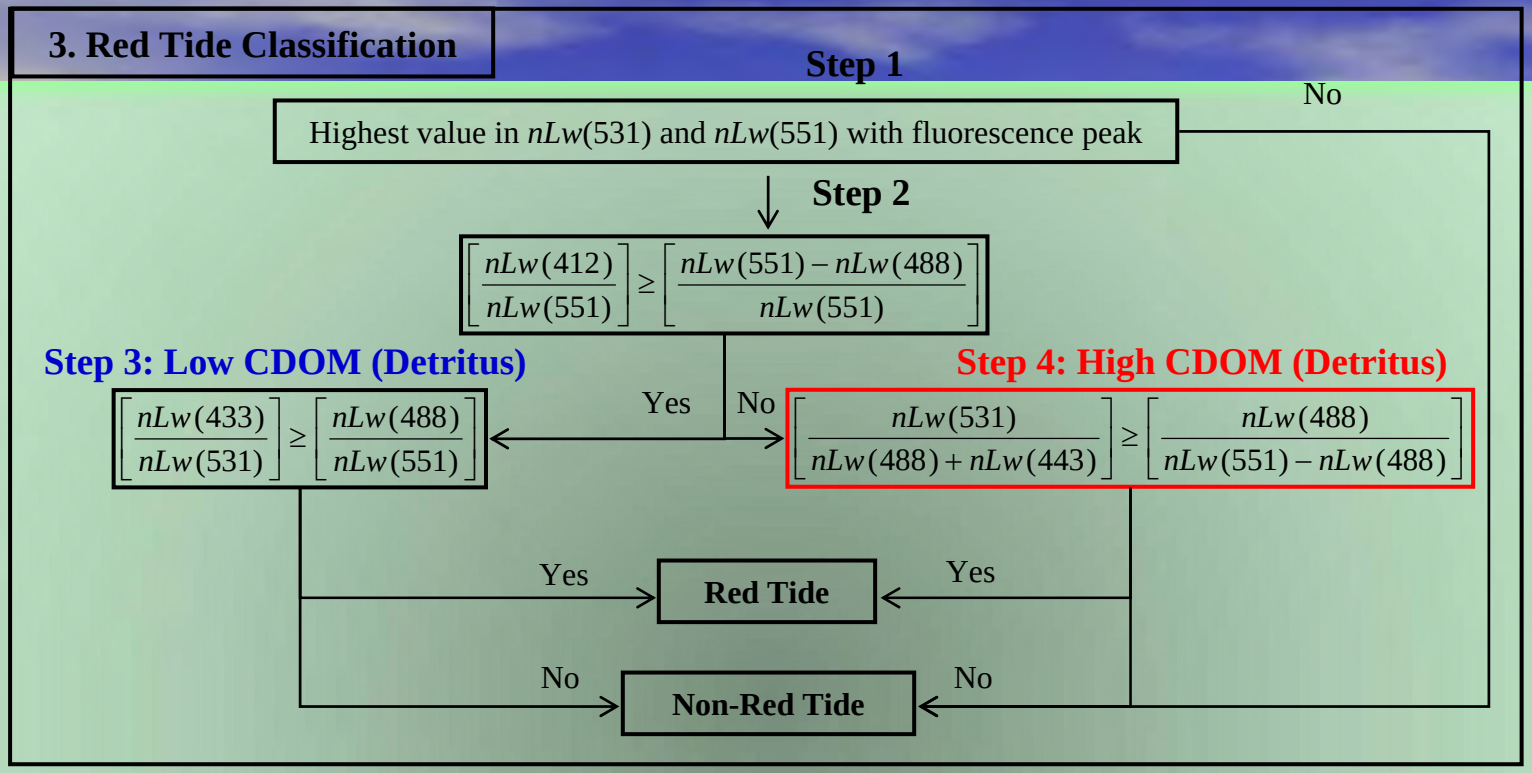

1. *C. polykrikoides* blooms :

- Onshore (high influence of CDOM or organic/inorganic material, increasing absorption in blue bands)

- Offshore (less influence of CDOM or organic/inorganic material, decreasing absorption and increasing water backscattering in blue bands).

2. Step 2 : Relatively high and low contribution of detritus/gelbstoff to chlorophyll

3. Step 3 : Lower contribution of CDOM to chlorophyll

4. Step 4 : Higher contribution of CDOM to chlorophyll

3. Results : High effect of Detritus/gelbstoff

Red Color :

$$\left[\frac{nLw(531)}{nLw(488)+nLw(443)}\right] \geq \left[\frac{nLw(488)}{nLw(551)-nLw(488)}\right]$$

Green Color :

$$\left[\frac{nLw(531)}{nLw(488)+nLw(443)}\right] < \left[\frac{nLw(488)}{nLw(551)-nLw(488)}\right]$$

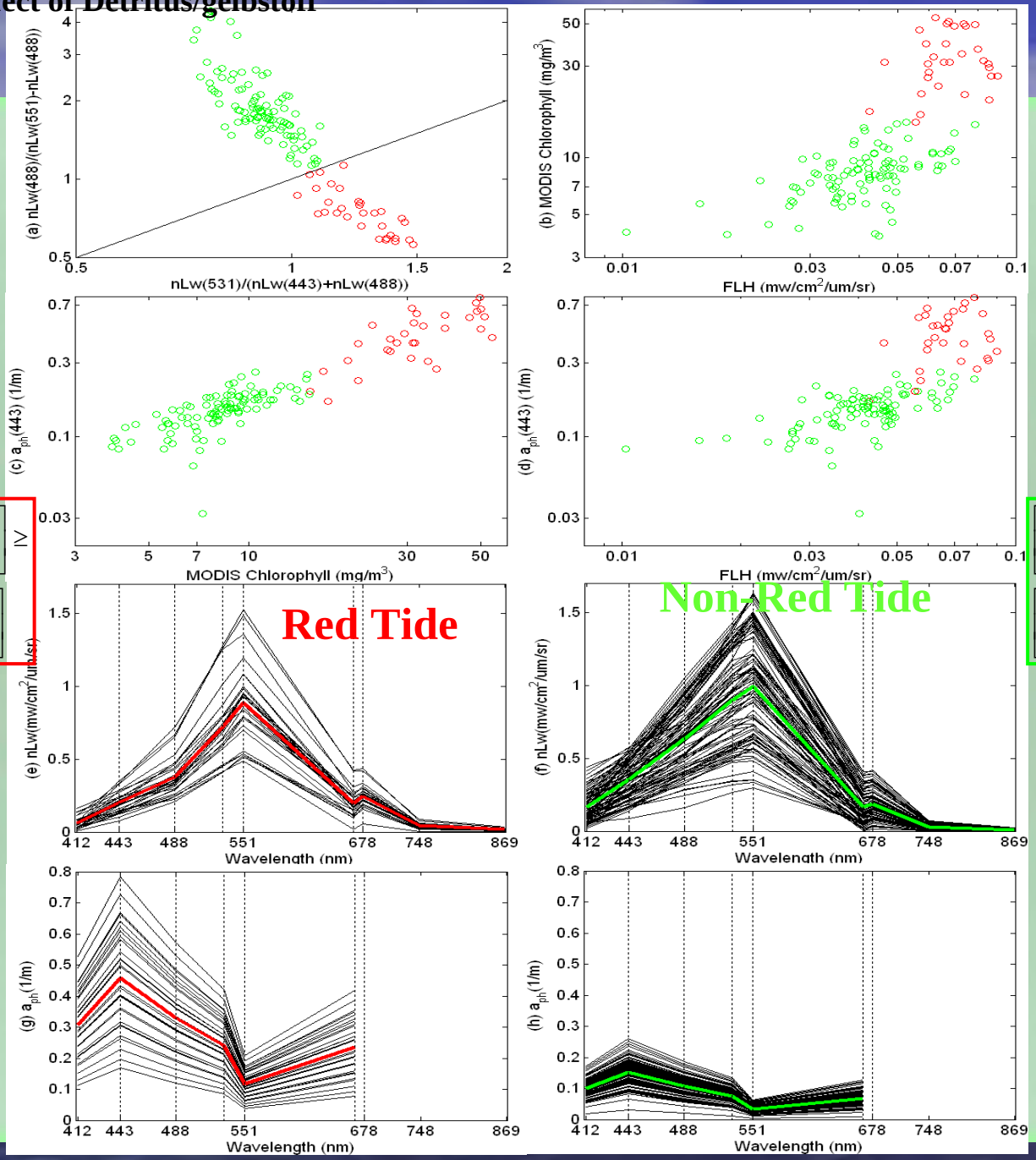

4. Discussions

Red Tide Difference between red and non-red tide **Non-Red Tide**

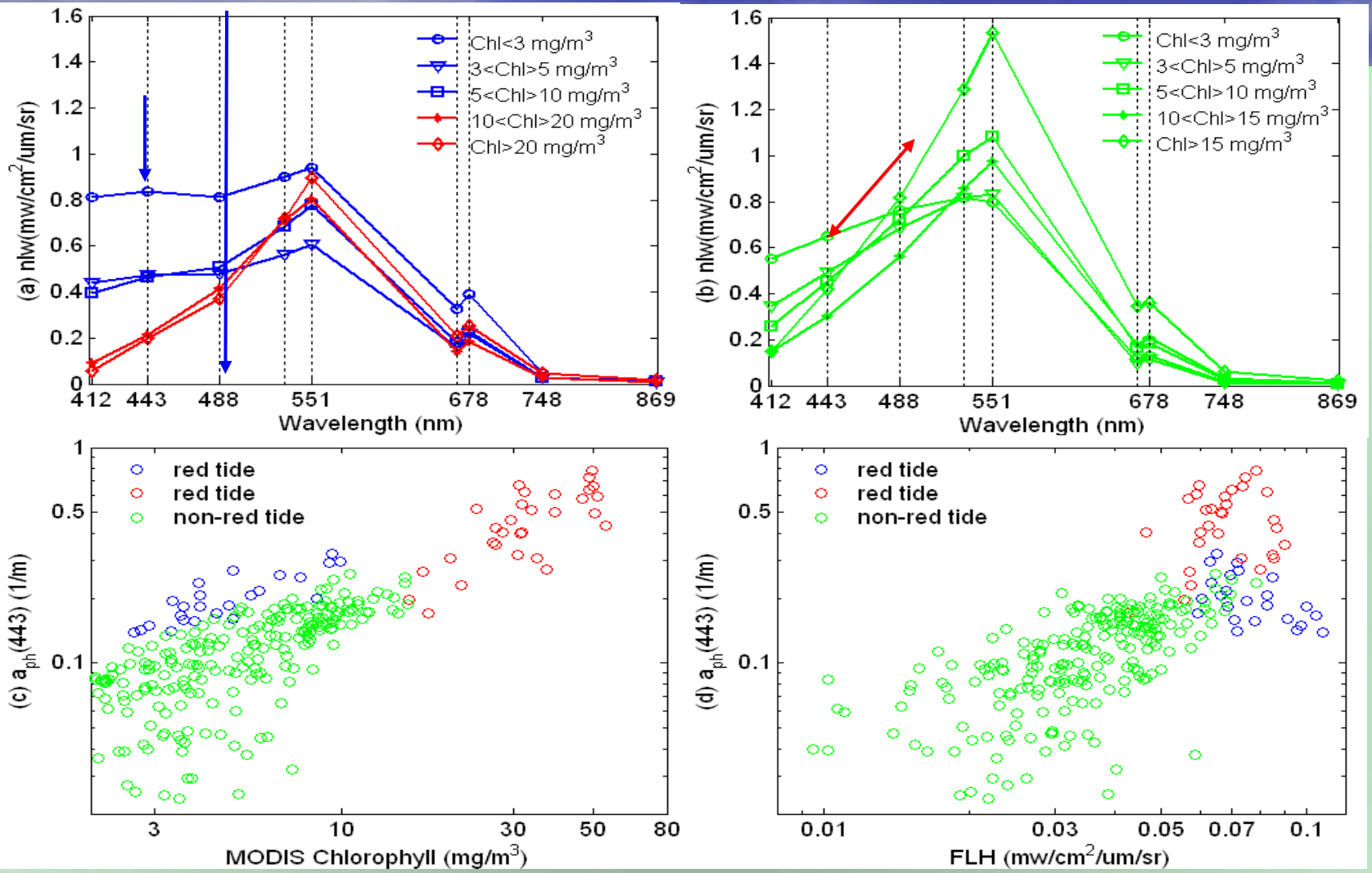

1. Blue bands : Increasing pigment absorption at 443 nm caused lower slope between blue and green bands.
2. Different radiance value at blue bands : the relative effect of CDOM per chlorophyll
3. Red tide waters are related to enhanced phytoplankton absorption and FLH with varying chlorophyll

Inshore showed the low salinity due to heavy rain
HAB move to offshore

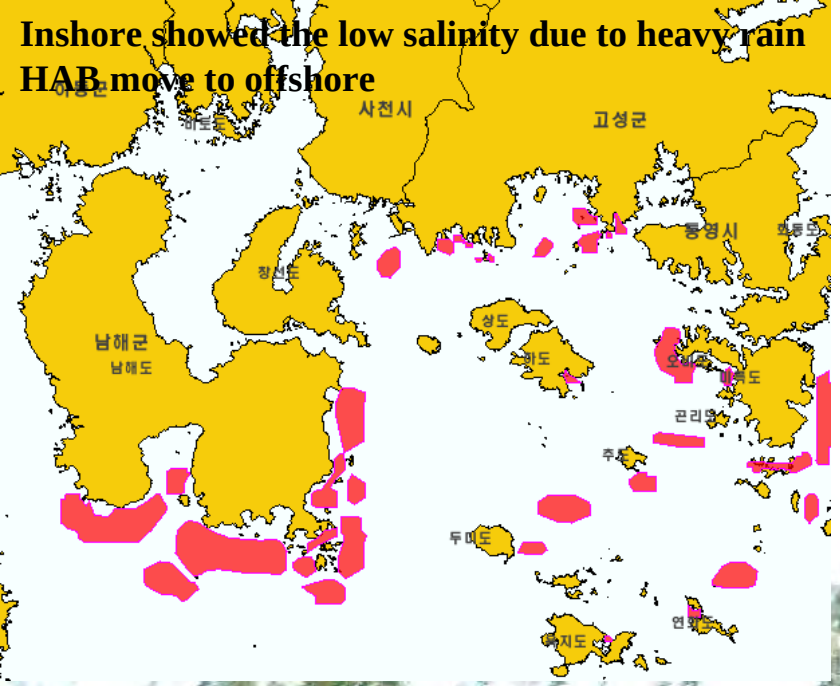

2002-08-19 (231)

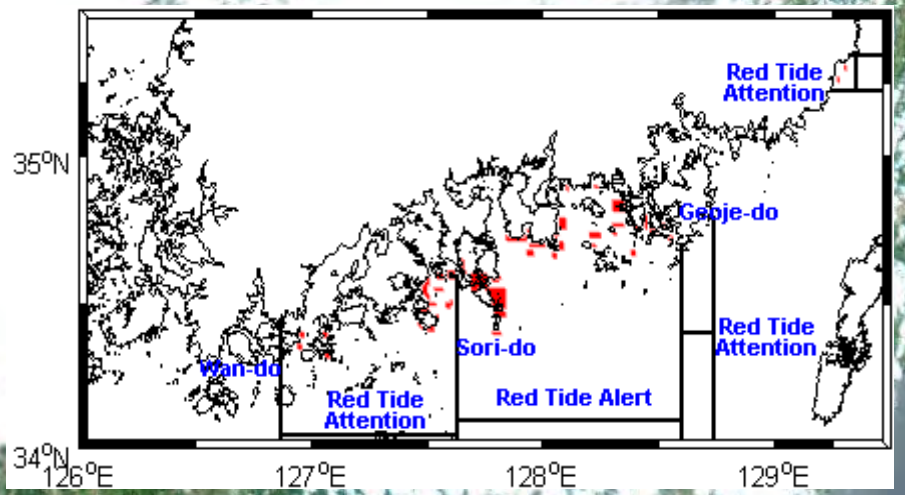

4. Discussions : Case Study

2002-08-19 (231)

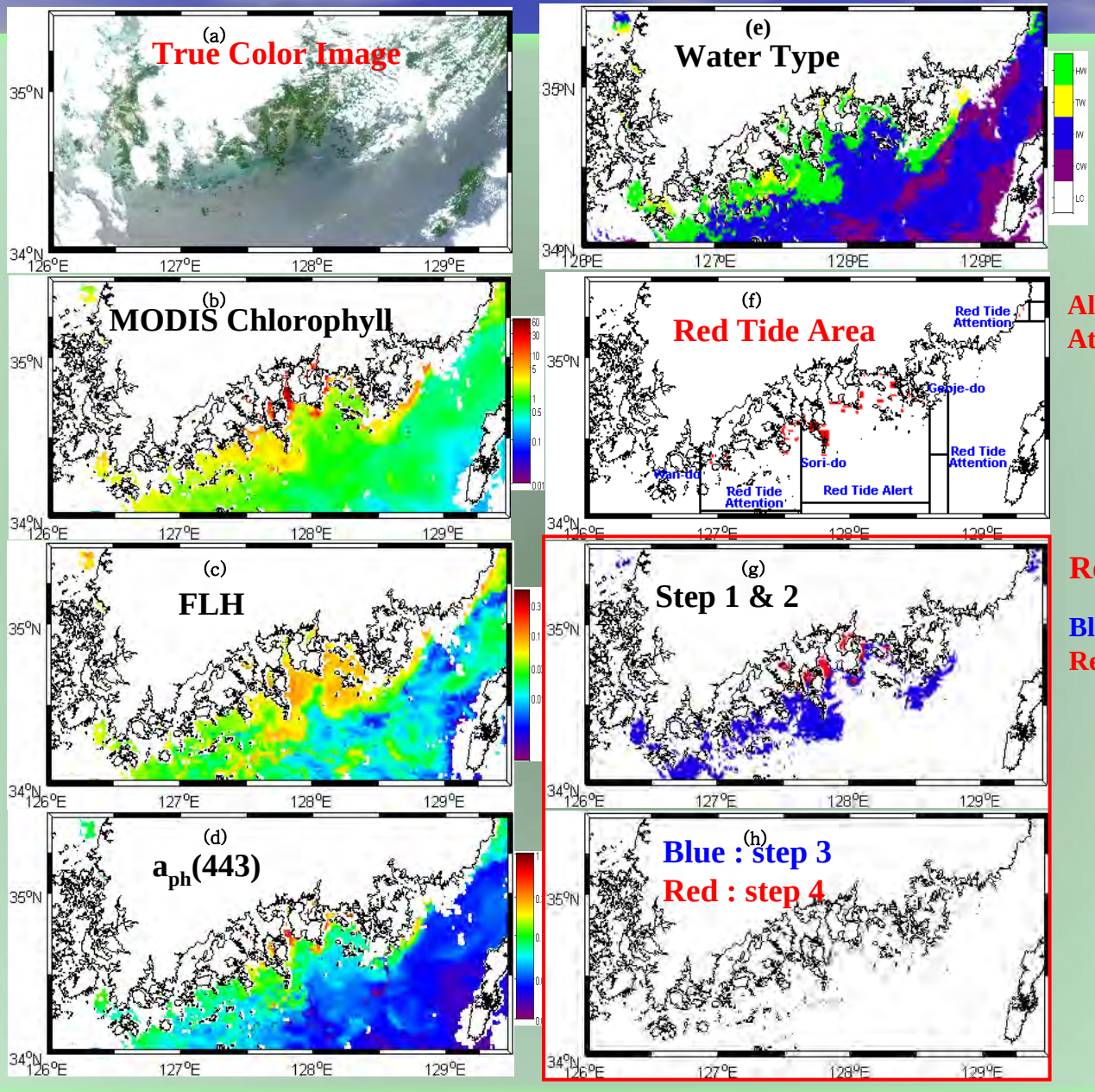

CW:22 (%)
IW :55 (%)
TW: 4 (%)
HW:19 (%)

Alert : > 1000 cells ml^{-1}
Attention : > 300 cells ml^{-1}

Red Tide Classification

Blue : low gelbstoff/detritus
Red : high gelbstoff/detritus

2002-09-08(251) – After Rusa

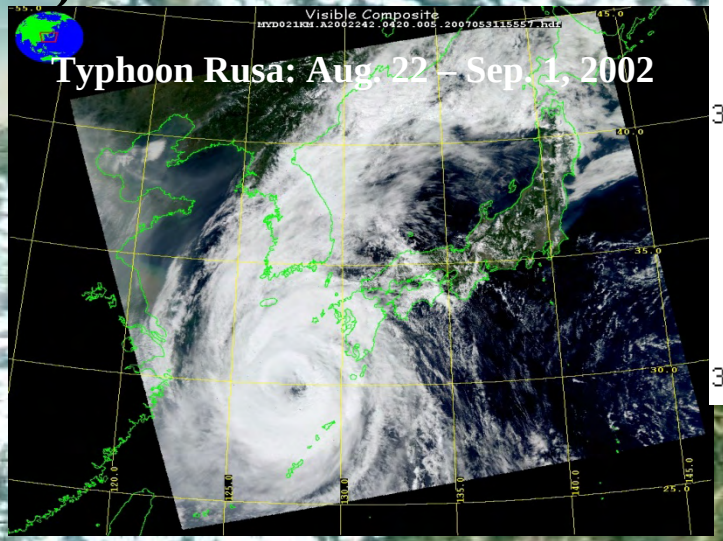

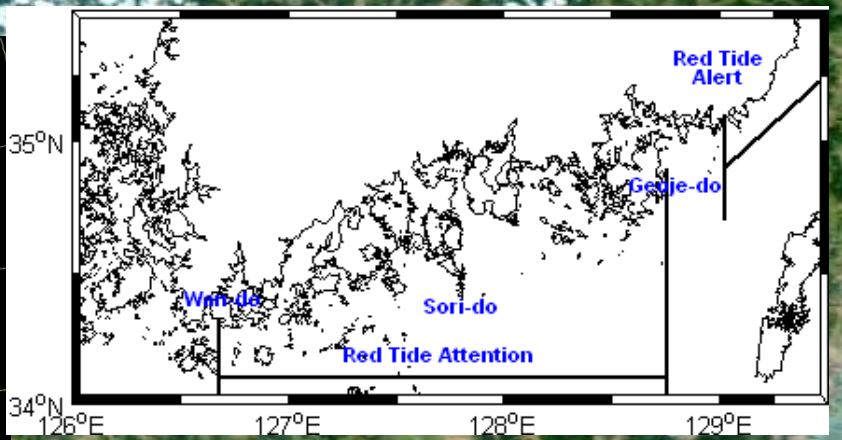

4. Discussions : Case Study 2002-09-08(251) – After Rusa

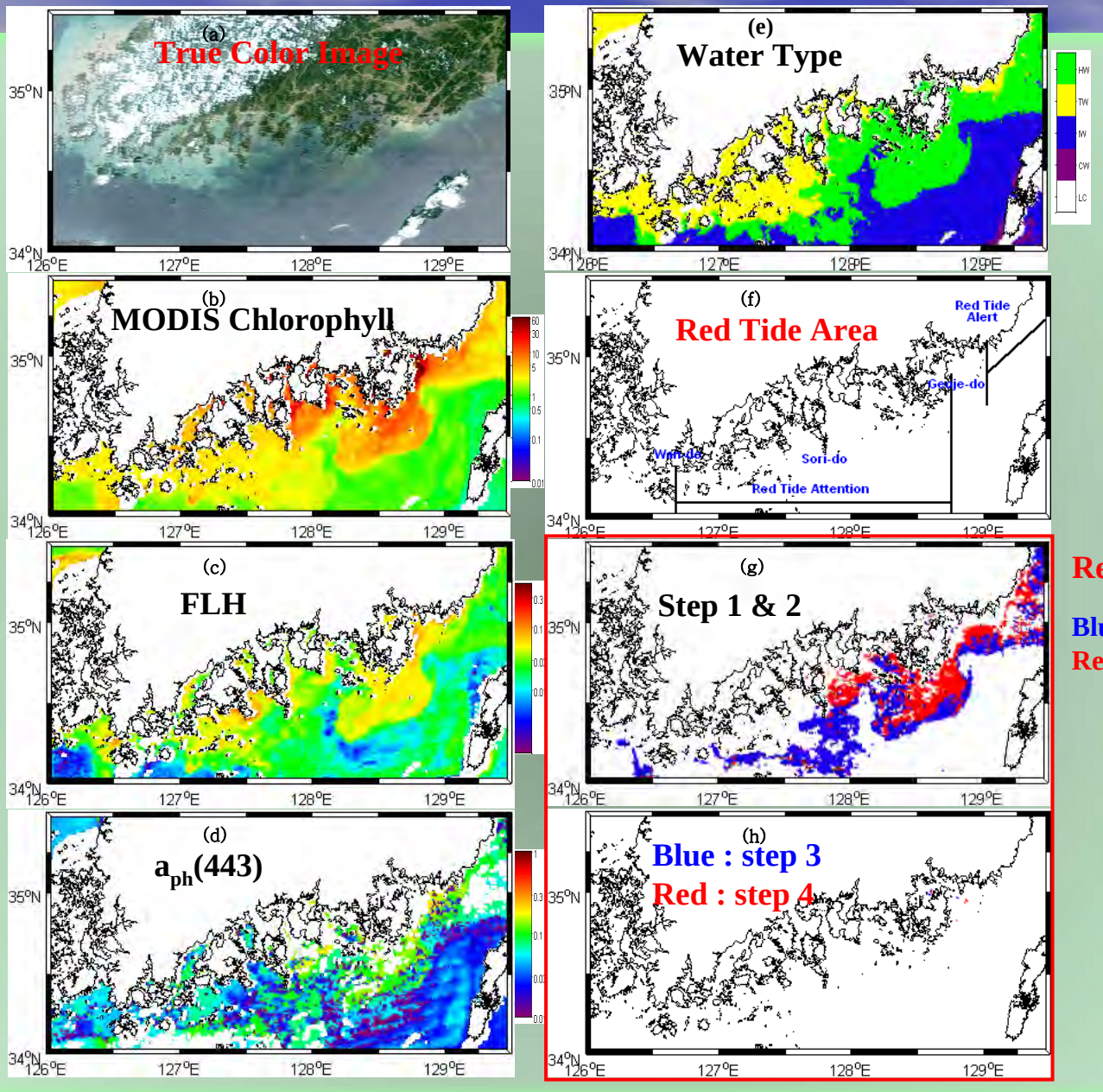

CW: 2 (%)
IW : 39 (%)
TW: 24 (%)
HW:35 (%)

Red Tide Classification

Blue : low gelbstoff/detritus
Red : high gelbstoff/detritus

5. Conclusions

1. For understanding of algal blooms at the South Sea of Korea, we developed a systematic method for classifying complicated coastal waters included red tide using MODIS remote sensing data.

2. We developed a spectral classification to test different optical water types across from high to low organic/inorganic particle concentrations as the clear, intermediate, turbid, mixed, and red tide water, which guided by different three criteria.

and to discriminate the red and non-red tide conditions, which guided by different four criteria.

3. *C. polykrikoides* blooms in SSK observed that radiance is higher at green bands and lower at blue bands due to the influence of strong pigment backscattering and high chlorophyll absorptions

4. Analysis of MODIS ocean color imagery revealed that pixel-based classification projected into distinct clusters in space domain, suggesting that this approach is promising for mapping phytoplankton blooms from various water conditions regionally based on remote sensing data.

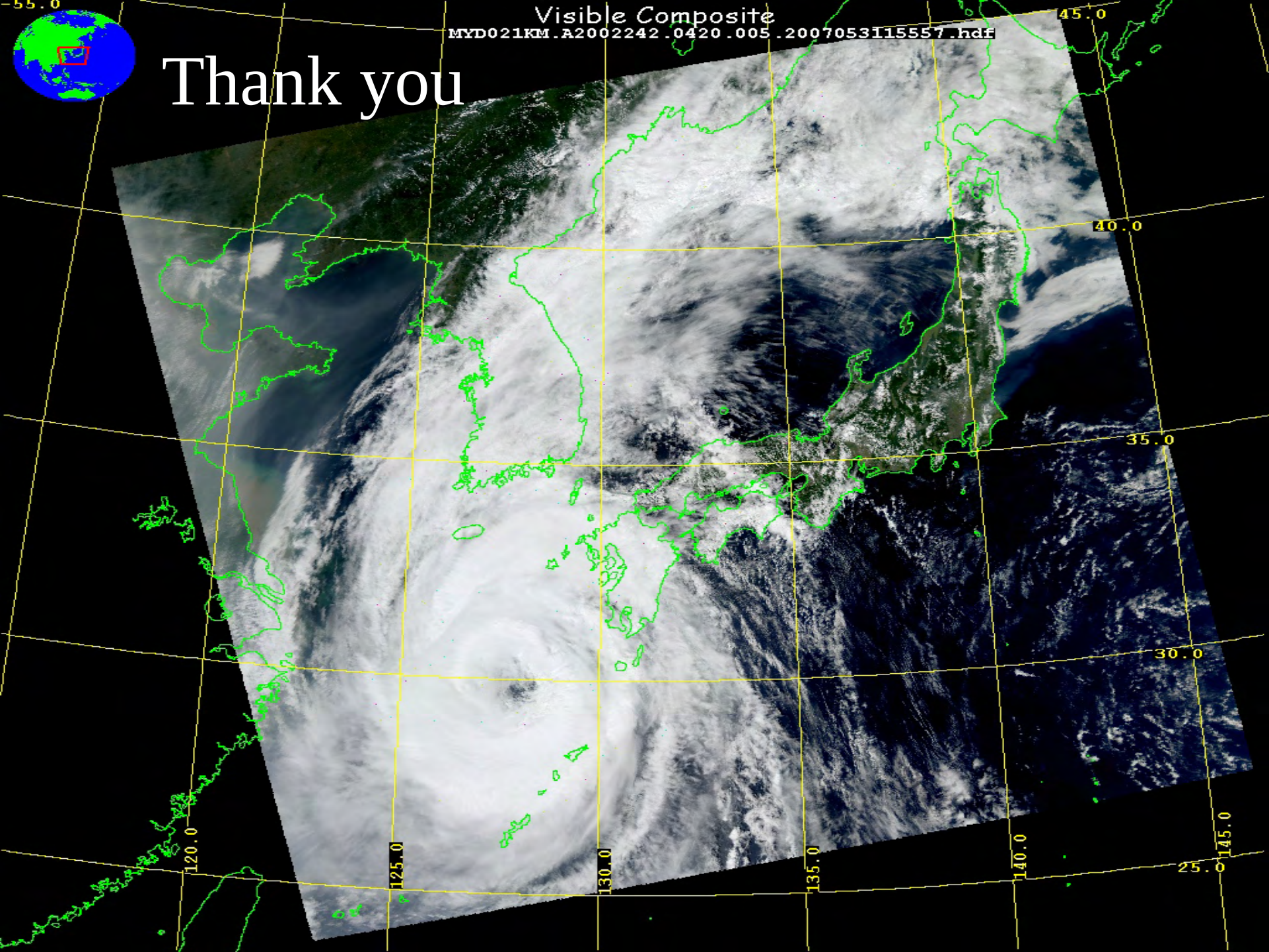
Visible Composite
MYD021KM.A2002242.0420.005.2007053115557.hdf
Thank you
55.0
45.0
40.0
35.0
30.0
25.0
120.0
125.0
130.0
135.0
140.0
145.0